Microstructural and Mechanical Characterization of Gas Metal Arc Welded AISI 430 Ferritic Stainless Steel Joints

Mustafa ŞENOL¹, Gürel ÇAM^{2*}

¹ Iskenderun Technical University, Institute of Graduate Studies, Department of Mechanical Engineering, 31200 iskenderun-Hatay, Turkey.

²Iskenderun Technical University, Faculty of Engineering and Natural Sciences, Department of Mechanical Engineering, 31200 İskenderun-Hatay, Turkey.

*Corresponding Author email: gurel.cam@iste.edu.tr

Abstract

Ferritic stainless steels contain Cr as the main alloying element and display very good corrosion resistance even at high temperatures. These steels are widely used in manufacturing of products such as hot water storage units, car chassis components, exhaust systems and kitchenware. The most characteristic difficulty in fusion joining of this type of stainless steels is the grain growth in the HAZ. Furthermore, martensite formation or carbide precipitation along the grain boundaries in the HAZ may also be observed if the heat input used is extremely high or C content of the steel and/or filler wire high. Thus, it is required that the heat input should be kept low or filler wires with low C should be used to successfully join these steels by conventional fusion welding methods. The determination of the effect of heat input on microstructural evolution in the weld region and the mechanical properties of the joints in gas metal arc welding of AISI 430 ferritic steel plates is aimed in this study. To that end, AISI 430 ferritic steel plates with a thickness of 5 mm were joined using different heat input values. The microstructures in the weld region and mechanical properties of the welded joints were determined by extensive optical microscopy investigations, microhardness measurements, tensile and bending tests. Moreover, the heat input effect on the joint performance was also studied.

Key words

Ferritic stainless steel, AISI 430, heat input, martensite formation, weld performance

1. INTRODUCTION

AISI 430 grade ferritic stainless steel (FSS) possesses high strength and corrosion resistance coupled with relatively low cost. In addition, ferritic stainless steels have more resistance to chloride stress corrosion cracking than austenitic stainless steels (ASS). Thus, it is widely used in a wide range of applications ranging from household utensils, vehicle exhausts, road and rail vehicles to other applications in several industries such as oil, gas, petrochemical, nuclear and power industries [1-10]. They are the second largest selling type of stainless steels behind austenitic grades.

The major problem encountered in welding of FSSs is the reduced ductility (toughness) in the heat affected zone (HAZ) which limits their application [2]. This problem is caused by the evolution of large grains in the HAZ of

fusion welds. The temperature in this region reaches a critical temperature (955 °C) and causes rapid growth of the ferrite grains [3]. Moreover, although the carbon content of FSSs is very small, on rapid cooling the formation of intergranular martensite and/or chromium-depleted zones may take place along the grain boundaries in HAZ. Formation of martensite in the HAZ even in small amounts results in a loss of ductility in addition to grain coarsening. Carbide precipitation can make the steel sensitive to inter-crystalline corrosion.

For instance, Aguilar et al. [6] investigated the metallurgical transformations occurring during the submerged arc welding (SMAW) of AISI 430 FSS with AISI 316L ASS using two different filler wires, namely E309L and E2209. They clearly demonstrated that both grain growth and martensite formation at the ferrite grain boundaries took place in the HAZ of 430 steel next to the fusion line in both joints. They also reported that a refined grain zone was present following the coarse grain zone in the BM side of the HAZ of 430 steel. Similarly, Antunes et al [8] investigated the effect of the weld metal on the microstructure and mechanical behaviour of FSS AISI 444 welded joints employing two types of filler metal of ASS, namely E309L and E316L. The microstructural examinations conducted showed that a grain coarsening occurred in the HAZ of both welded joints. A recent study indicated that duplex SS consumables such as E2204 can be used to obtain defect-free welds of FSS. Duplex SS consumables can also yield higher strength than ASS consumables [9]. Moreover, Zhou et al [7] studied the influence of heat input on microstructural and mechanical characteristics of AISI 430 FSS joints produced by cold metal transfer GMA welding using E308L filler wire. They observed that the carbide precipitation and the formation of intergranular martensites as well as the coarsening of ferrite grains occurred in the coarse-grained zone of HAZ. They also reported that increasing heat input also caused an increase in the amount of intergranular martensite and carbide precipitation.

Heat input is a very important weld parameter in joining of FSSs. Thus, a low heat input solid state welding technique, namely friction stir welding, which was originally developed for low melting temperature Al-alloys [11-20] as well as Cu-alloys [21-23] and Pb [24], has a potential to join steels including stainless steels [25,26]. Similarly, low heat input CMT arc welding method [12,27] or power beam welding techniques [28-33] also offers a potential to join these steels. As a result, several studies have been conducted on FSW of steels including SSs in last 30 years [26,27,34-41]. However, it was observed that wear of the stirring tool takes place in FSW of steels since a peak temperature may reach over 1000 oC. Thus, even the tools made of high temperature resistant materials may wear slowly over the time.

Furthermore, extra low C, Ti or Nb containing FSS grades have been developed in recent years to overcome carbide precipitation and martensite formation along the ferrite grain boundaries within the HAZ. However, it is usually required to keep the heat input as low as possible to avoid grain growth within the HAZ next to the fusion line. Thus, the use of a low heat input (1kj/mm) and an interpass temperature of maximum 100-120°C is recommended in welding of these steels. Moreover, preheat is not advisable although it may be helpful when welding sections over 10mm thick, where excessive grain growth and welding restraint may result in cracking of the joint. Although preheating will lead to grain growth, it will reduce the cooling rate experienced in the HAZ. Thus, this will keep the FZ temperature above the ductile-brittle transition point and may reduce residual stresses. Preheat temperatures should be, however, kept between 50-250 °C depending on the composition of the steel.

In this study, the weldability of FSS, namely AISI 430, and the influence of heat input applied to the plates on the microstructural evolution in the joint area and thus on joint properties were investigated. Thus, 5 mm thick AISI 430 plates were welded by gas metal arc welding (GMAW) using a filler wire of ER307 with a diameter of 1.2 mm. Detailed microstructural investigations were conducted for microstructural characterization of the joints and detailed microhardness measurements were carried out in addition to the mechanical tests to determine the joint properties. Moreover, the influence of heat input on the microstructure in the joint area and thus on the joint performance was evaluated.

2. MATERIALS AND METHOD

In this study, AISI 430 grade FSS plates with a thickness of 5 mm were used. It was received in the form of large plate with the sizes of 1500x1000x5 mm3. Its composition is illustrated in Table 1.

Chemical Composition (wt. %)										
Material	C	Si	Mn	P	S	Cr	Ni	N	Mo	Cu
Base Material (AISI 430)	0,037	0,38	0,50	0,031	0,002	16,16	0,27	0,033	0,01	0,20
Filler Material (ER307)	0,075	0,790	7,10	0,009	0,020	19,075	9,010		0,005	0,070

Table 1. Composition of AISI 430 grade austenitic steel plates used in this study.

Rectangular pieces with the sizes of 250x190 mm were extracted from the as-received large plate and welding grooves were machined as illustrated in Fig. 1, prior to welding. The surfaces to be joined were cleaned mechanically using a stainless steel metal brush prior to the joining process. GMAW welding was carried out in two passes using an ER307 filler wire of 1.2 mm in diameter, the feeding rate was 17,5 mm/s. The weld parameters employed in welding trials were given in Table 2. As seen from this table, the welding trials were conducted using two different heat inputs in order to determine how the joint performance is influenced by heat input.

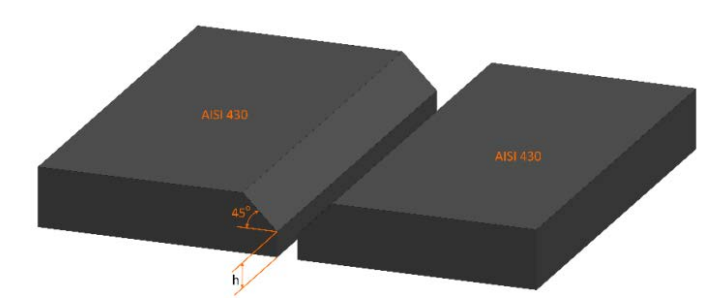


Figure 1. Preparation of the plates for welding trials.

Weld Trial	Current	Voltage	Weld speed	Feeding rate of	Shielding gas	
	(A)	(V)	(mm/s)	filler wire (mm/s)		
Low Heat Input	ave. 385	28	4,5	17,5	Argon (99,95%)	
High Heat Input	ave. 465	27	4,0	17,5	Argon (99,95%)	

Table 2. The process parameters employed in welding.

One metallography specimen, two bend specimens and four tensile specimens were extracted from each joint in order to investigate the microstructural evolutions in the weld regions of the joints produced and to evaluate its influence on the mechanical properties. For comparison purposes and to evaluate the joint performance, four tensile specimens were also extracted from the base plate. The metallography specimens were first ground and polished prior to etching in which the specimens were immersed in a solution comprising of 50 ml HCl and 150 ml HNO3 for about 17 seconds. A detailed microstructural investigations were carried out on these specimens as well as microhardness measurements. Microhardness measurements were done on each joint along three lines across the weld region, using a load of 500 g, as schematically illustrated in Fig. 2.

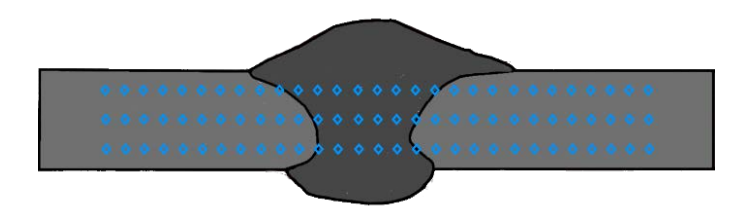


Figure 2. Schematic showing the conduction of microhardness measurements on each joint along three lines across the weld region.

Moreover, tensile test specimens of both the BM and the joints were tested with a loading rate of 15 mm/s to evaluate the mechanical properties, joint performance values and the weld qualities. Two bend specimens were also extracted from each joint in order to determine whether cracking occurs in the weld region of the joints produced using different heat input values. One of them was bent in the condition of surface bend and the other in the root bend configuration. The specimens were bent about 180 degrees and the weld center in the middle

position. Furthermore, the influence of heat input on the microstructural evolution in the HAZ and thus on mechanical behavior of the joints was also determined.

3. RESULTS AND DISCUSSION

The results obtained from this study will be discussed below in two subsections.

3.1. Microstructural Aspects

Figure 4 (a) shows the microstructure of the BM used in this study. The BM microstructure consists of a fully ferritic microstructure containing carbides, which are evenly distributed within the grains as well as along the grain boundaries. Figure 3 and 4 give macrograph and micrographs illustrating the weld cross-sections of the joints and the microstructures observed in the HAZ and FZ of the joints produced using low and high heat inputs, respectively. As seen from the micrographs, a fine dendritic structure was observed in the FZ of both joints. However, the grain size of dendritic structure is slightly coarser in the high heat input joint (Fig. 4c). This is not unexpected since high heat input applied during welding results in grain growth in the FZ.

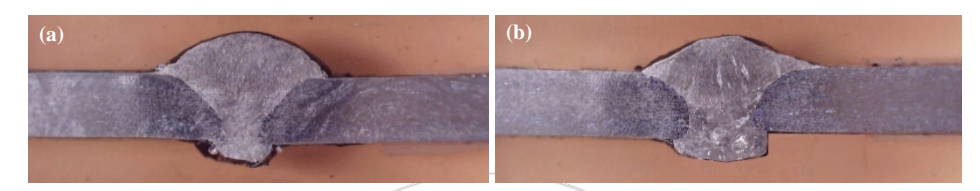


Figure 3. The macrographs illustrating the weld cross-sections of the welds produced: (a) the lower and (b) the higher heat input joint.

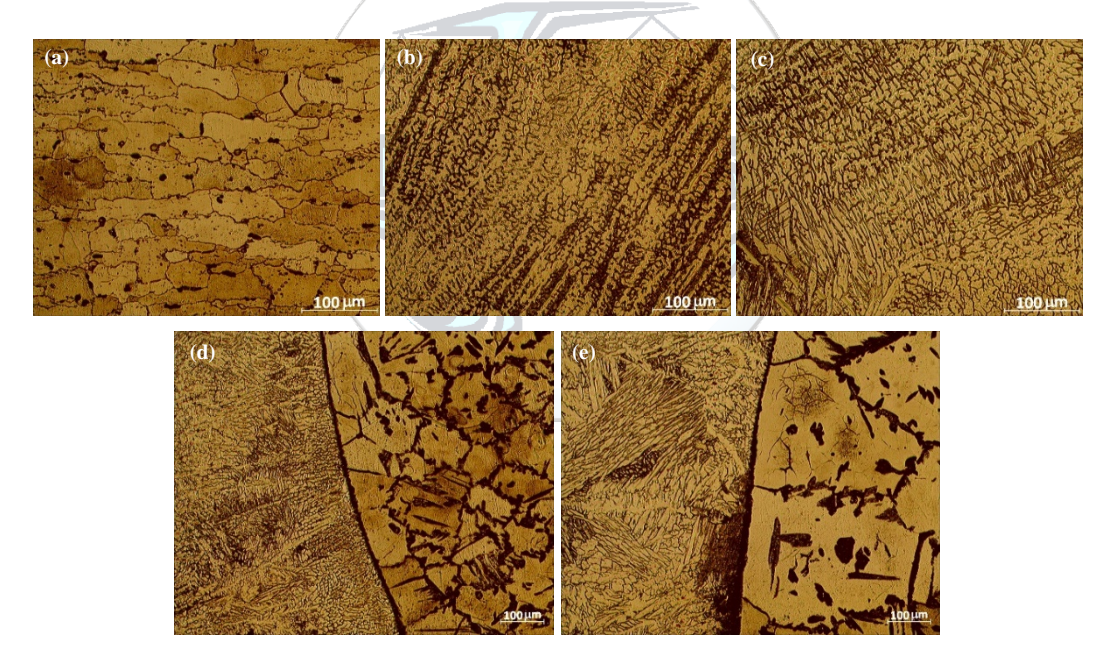


Figure 4. The micrographs illustrating the microstructures of: (a) BM, (b) and (c) FZ of the lower and higher heat input joint, respectively, and (d) and (e) HAZ of the lower and higher heat input joints, respectively.

Furthermore, it was observed that the BM microstructure was affected by solid state phase transformations induced by the weld thermal cycle in the HAZ of both joints. Thus, two distinct HAZ regions were formed in both joints, namely high temperature HAZ (so-called coarse grained HAZ, i.e. FGHAZ) and low temperature HAZ (often referred to fine grained HAZ, i.e FGHAZ) which is on the base metal (BM) side. Although both joints did exhibit CGHAZ next to the fusion boundary (FB), the extent of grain growth is much higher in the high heat input joint as clearly seen from Figs. 4(d) and (e). Martensite formation along the grain boundaries of ferrite phase and the growth of ferrite grains were detected in the HAZ region. Moreover, carbide precipitation along the fusion boundary was also observed in both joints. The grains were clearly much finer in the FGHAZ, and the grain size was almost the same as that of the BM, in contrast to CGHAZ where the grains are much coarser. Moreover, the evolution of intergranular martensites was also observed in the FGHAZ. However,

compared with CGHAZ, the amount of martensite was significantly less, and the martensite distributed discretely at the grain boundaries and no longer formed within the grains. The reason for this is the fact that the fine grain zone is far away from the FZ and the temperature is low. Thus, the formation of high-temperature austenite is suppressed, which inhibits martensite formation. The content of intergranular martensite and carbide precipitates along the fusion boundaries increases with an increase in heat input. Thus, the width of the HAZ also increases slightly with increasing heat input. According to Khorrami et al [42], the martensite formation in the HAZ of medium-Cr FSS joint is a well-known phenomenon. Van Warmelo et al [43] also proposed that the precipitates of carbides, nitrides or carbonitrides were usually formed in the HAZ of FSS. Moreover, Zou et al [7] reported that the dominant precipitate was Cr-rich carbide, i.e., M23C6 in which 'M' mostly stands for Cr and Fe. However, there is no clear indication of these precipitations in the HAZ of 430 FSS joints in the current study.

3.2. Mechanical Properties

Figure 5(a) and 5(b) gives the hardness profiles obtained from the joints produced using low and high heat inputs. These hardness profiles show the hardness variations across the joints. As clearly seen from these profiles, both joints displayed similar hardness variations across the weld region. The hardness profiles clearly show that there is a hardness increase (strength overmatching) in the weld region for both joints, particularly in the HAZ region. Thus, both joints display a typical hardness profile of strength overmatching joints. This hardness increase in the weld region of both joints is due to the formation of fine dendritic microstructure in the fusion zone (FZ) and the formation of intergranular martensite and growth of ferrite grains in the HAZ. Furthermore, the width of the HAZ in which hardness variation took place is wider in the higher heat input joint, indicating that the higher heat input has a significant effect on microstructure and thus on hardness across the weld region.

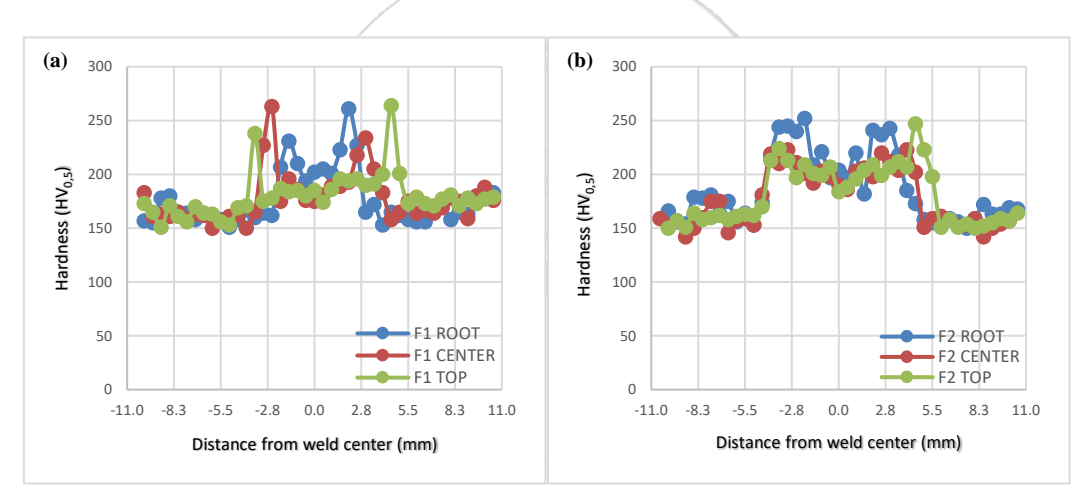


Figure 5. Hardness variation across the joints: (a) the lower heat input joint and (b) the higher heat input joint.

The results of tensile tests performed on the specimens of the BM and the joints produced using different heat input values are summarized in Table 3 and shown in Figure 6-7. Both welded joints showed good tensile strength and the failure took place at the BM away from the FZ for all samples. The tensile strength of both joints were very similar to that of the BM, Fig. 7. Thus, the tensile strength performance of both joints was found to be as high as 99%. On the other hand, both joints displayed lower ductility; i.e. about 15%, than that of the BM, i.e. 23%. This is not surprising since there is a strength overmatching in both joints as clearly illustrated by the hardness profiles. Thus, the higher strength weld region stays in the elastic region and does not contribute to the total elongation. This confined plasticity occurring only in the base plate sides of the tensile test specimen results in decreasing of the percentage elongation value. Similar results were also reported inhomogeneous welded joints, namely strength overmatched laser beam welded steels [28-30], strength undermatching Al-alloys joints [44-49] and bi-metallic joints showing confined plasticity [50,51]. Moreover, all the tensile specimens of the joints failed in the BM (in the region between fine grained HAZ and the base metal), as shown in Figure 8.

In contrast to tensile testing, the heat input variation employed in this study affected the joint behavior in bend testing. Although no cracking occurred in both surface and root bend specimens extracted from the lower heat input joint, the root bend specimen of the higher heat input joint has cracked as shown in Figures 9 and 10. The reason for this cracking is due to the presence of very coarse grains as well as martensite formation in the HAZ region next to the fusion line diminishing the toughness in this area (Fig. 4e).

Specimen	R _{P0.2} (MPa)	R _m (MPa)	Elongation (%)	Strength Performance (%)	Ductility Performance (%)	Failure Location
Base Plate	396, 392, 395 (394)	506,501,504 (504)	21, 25, 22 (23)			
Low Heat Input Joint	358, 364, 348, 354 (356)	498, 496, 495, 499 (497)	14, 15, 15, 15 (15)	99	65	Base plate
High Heat Input Joint	352, 300, 342, 341 (335)	497,496, 498, 503 (499)	15, 16, 14, 15 (15)	99	65	Base plate

Table 3. Tensile test results.

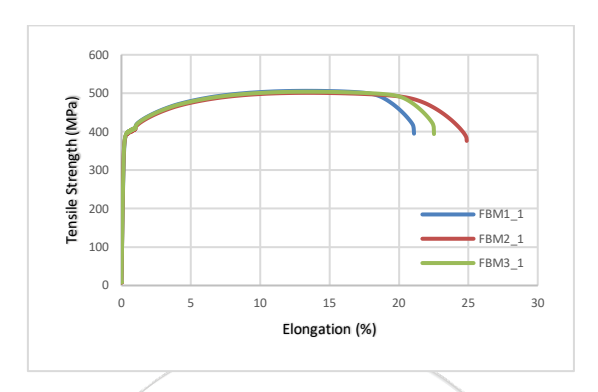


Figure 6. Stress-elongation (%) curve of the base plate AISI 304 steel used.

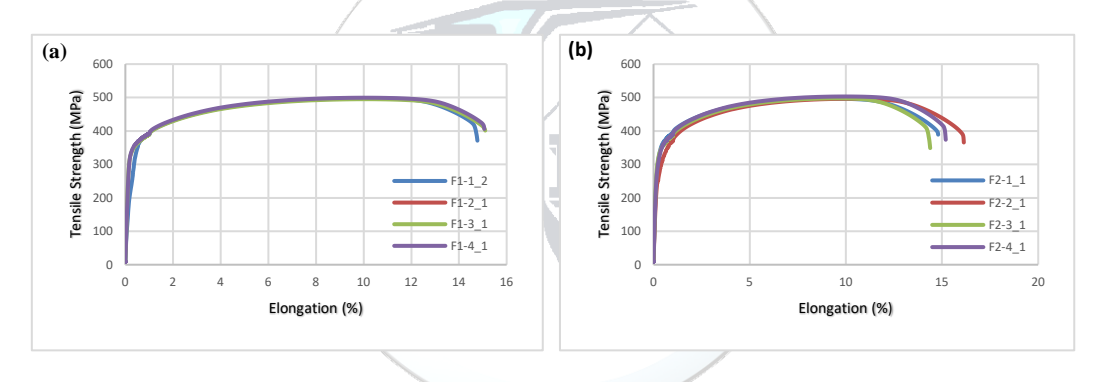


Figure 7. Stress-elongation (%) curves of: (a) lower heat input joint, and (b) higher heat input joint.

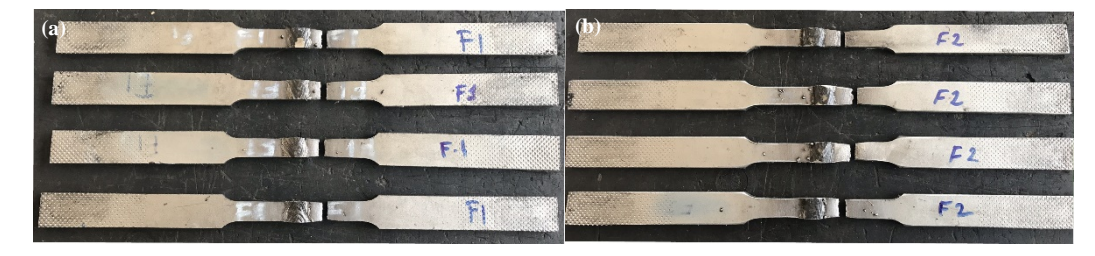


Figure 8. Macrographs showing the fracture locations in the tensile test specimens extracted from: (a) lower heat input joint and (b) higher heat input joint.

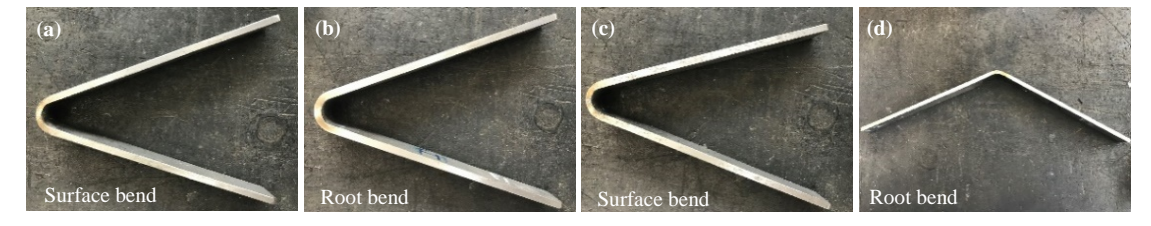


Figure 9. Macrographs showing the surface and root bend specimens extracted from: (a) lower heat input joint and (b) higher heat input joint. Note that no cracking occurred in any of the specimens.



Figure 10. Macrograph showing the failure location in root bend specimens extracted from the higher heat input joint. Note that failure takes place in the coarse grained HAZ (CGHAZ) region.

4. CONCLUSIONS

The weldability of AISI 430 plates with a thickness of 5 mm by GMAW welded using a filler wire of 307 with a diameter of 1.2 mm and the influence of heat input on the microstructural evolution in the joint area and thus on joint properties were investigated. The following conclusions were withdrawn from this study:

- AISI 430 plates with a thickness of 5 mm was defect-free welded in two passes by GMAW process.
- A fine dendritic microstructure was evolved in the fusion zone of both joints, although the grain size of the dendrites was slightly coarser in the higher heat input joint.
- Two distinct HAZ regions were formed in both joints namely coarse grained HAZ (CGHAZ) and fine grained HAZ (FGHAZ) regions.
- It was observed that the martensite formation along ferrite grain boundaries (intergranular martensites) and the coarsening of ferrite grains took place in the CGHAZ. However, no martesite was observed along the grain boundaries in the CGHAZ next to the fusion boundary. On the contrary, carbide precipitation was observed along the fusion boundaries of both joints.
- Both joints displayed a hardness increase in the weld region.
- All the tensile test specimens failed in the base plate. Both joints showed similar strength values to that of the BM, the strength performance of the joints being about 99%. However, the ductility performance was lower, i.e. about 65%, due to confined plasticity resulting from strength overmatching weld region. No clear indication of the influence of the heat input on joint performance has been observed in tensile loading condition.
- Both surface and root bend specimens extracted from lower heat input joint did not crack in bending test while the surface bend specimen did not crack but root bend specimen failed in the case of higher heat input joint, indicating that the heat input variation did in fact affect the joint behavior in bending condition. The results also indicate that the strength overmatching weld region cannot shield the cracking in root bend condition in the case of higher heat input joint.

ACKNOWLEDGMENT

We would like to thank Mr. Sedat UYSAL and Tuğrul YAZGAN from NOKSEL Çelik Boru Sanayi A.Ş. (Noksel Steel Pipe Inc.), İskenderun-Hatay, Turkey, for their support in conduction of the metallography and mechanical tests. The authors also thank Hikmet Gizem SARSILMAZ from Kahraman-Sarsılmaz Machinery, İskenderun, for conducting welds.

CONFLICT OF INTEREST STATEMENT

The authors declare that there is no conflict of interest.

REFERENCES

- [1]. N. Ghosh, P.K. Pal, G. Nandi, "GMAW dissimilar welding of AISI 409 ferritic stainless steel to AISI 316L austenitic stainless steel by using AISI 308 filler wire", *Engineering Science and Technology*, an *International Journal*, vol. 20, pp. 1334–1341, 2017.
- [2]. T. Mohandas, M.G. Reddy, M. Naveed, "A comparative evaluation of gas tungsten and shielded metal arc welds of a ferritic stainless steel", *J. Mater. Process. Technol.*, vol. 94, pp. 133-140, 1999.

- [3]. C. Lippold and D.J. Kotecki, Welding Metallurgy and Weldability of Stainless Steels. 1st ed., Hoboken: John Wiley & Sons Inc.; 2005.
- [4]. F.B. Pickering, "Physical metallurgy of stainless steel development", *Int. Met. Rev.*, vol. 21, pp. 227-268, 1976.
- [5]. R. Ghasemi, B. Beidokhti, M. Fazel-Najafabadi, "Effect of delta ferrite on the mechanical properties of sissimilar ferritic-austenitic stainless steel welds", *Arch. Metall. Mater.*, vol. 63 (1), pp. 437-443, 2018.
- [6]. S. Aguilar, R. Tabares, C. Serna, "Microstructural transformations of dissimilar austenite-ferrite stainless steels welded joints", *Journal of Materials Physics and Chemistry*, vol. 1 (4), pp. 65-68, 2013.
- [7]. J. Zhou, J. Shen, S. Hu, G. Zhao, Q. Wang, "Microstructure and mechanical properties of AISI 430 ferritic stainless steel joints fabricated by cold metal transfer welding", *Materials Research Express*, vol. 6 (11), Article No: 116536, 2019.
- [8]. P.D. Antunes, et al., "Mechanical and microstrutural characterization of weldments of ferritic stainless steel AISI 444 using austenitic stainless steels filler metals". *J. ASTM International*, vol. 9 (2), pp. 1-9, 2012.
- [9]. K. Shanmugam, A.K. Lakshminarayanan and V. Balasubramanian, "Tensile and impact properties of shielded metal arc welded AISI 409M ferritic stainless steel joints", *J. Mater. Sci. Technol.*, vol. 25 (2), pp. 181-186, 2009.
- [10]. A.K., Lakshminarayanan, "Effect of welding processes on tensile and impact properties, hardness and microstructure of AISI 409M ferritic ftainless joints fabricated by duplex stainless steel filler metal", *Journal of Iron and Steel Research, International*, vol. 16., pp. 66-72, 2009.
- [11]. N. Kashaev, V. Ventzke, and G. Çam, "Prospects of laser beam welding and friction stir welding processes for aluminum airframe structural applications", *Journal of Manufacturing Processes*, vol. 36, pp. 571-600, 2018.
- [12]. G. Çam and G. İpekoğlu, "Recent developments in joining of aluminium alloys", *Int. J. Adv. Manuf. Technol.*, vol. 91(5-8), pp. 1851-1866, 2017.
- [13]. G. Çam, "Friction stir welding (FSW) A novel welding technology developed for Al-Alloys", *Engineer and Machinery*, vol. 46 (541), pp. 30-39, Feb. 2005. (in Turkish)
- [14]. A. Von Strombeck, G. Çam, J.F. Dos Santos, V. Ventzke, and M. Koçak, "A comparison between microstructure, properties, and toughness behavior of power beam and friction stir welds in Al-alloys", in Proc. of the TMS 2001 Annual Meeting Aluminum, Automotive and Joining (New Orleans, Louisiana, USA, February 12-14, 2001), eds: S.K. Das, J.G. Kaufman, and T.J. Lienert, pub.: TMS, Warrendale, PA, USA, pp. 249-264, 2001.
- [15]. G. Çam, V. Javaheri, and A. Heidarzadeh, "Advances in FSW and FSSW of Dissimilar Al-Alloy Plates", *Journal of Adhesion Science and Technology*, 2022 (DOI: https://doi.org/10.1080/01694243.2022.2028073).
- [16]. G. İpekoğlu, B. Gören Kıral, S. Erim, and G. Çam, "Investigation of the effect of temper condition friction stir weldability of AA7075 Al-alloy plates", *Mater. Tehnol.*, vol. 46 (6), pp. 627-632, 2012.
- [17]. G. İpekoğlu, S. Erim, B. Gören Kıral, and G. Çam, "Investigation into the effect of temper condition on friction stir weldability of AA6061 Al-alloy plates", *Kovove Mater.*, vol. 51 (3), pp. 155-163, 2013.
- [18]. G. Çam, G. İpekoğlu, and H. Tarık Serindağ, "Effects of use of higher strength interlayer and external cooling on properties of friction stir welded AA6061-T6 joints", *Sci. Technol. Weld. Join.*, vol. 19 (8), pp. 715-720, 2014.
- [19]. G. Çam, S. Güçlüer, A. Çakan, and H.T. Serindağ, "Mechanical properties of friction stir butt-welded Al-5086 H32 plate", *Mat.-wiss. u. Werkstofftech.*, vol. 40 (8), pp. 638-642, 2009.
- [20]. A. Heidarzadeh, et al., "Friction stir welding/processing of metals and alloys: A comprehensive review on microstructural evolution", *Progress in Materials Science*, vol. 117, Paper No. 100752, 2021.
- [21]. T. Küçükömeroğlu, E. Şentürk, L. Kara, G. İpekoğlu, and G. Çam, "Microstructural and mechanical properties of friction stir welded nickel-aluminum bronze (NAB) alloy", *Journal of Materials Engineering and Performance (JMEPEG)*, vol. 25 (1), pp. 320-326, 2016.
- [22]. G. Çam, S. Mistikoglu, and M. Pakdil, 'Microstructural and mechanical characterization of friction stir butt joint welded 63%Cu-37%Zn brass plate', *Weld. J.*, vol. 88 (11), pp. 225s-232s, 2009.
- [23]. G. Çam, H.T. Serindağ, A. Çakan, S. Mıstıkoğlu, and H. Yavuz, 'The effect of weld parameters on friction stir welding of brass plates', *Mat.-wiss. u. Werkstofftech.*, vol. 39 (6), pp. 394-399, 2008.1997.
- [24]. A. Günen, E. Kanca, M. Demir, F. Çavdar, S. Mistikoğlu, and G. Çam, "Microstructural and mechanical properties of friction stir welded pure lead", *Indian Journal of Engineering & Materials Sciences (IJEMS)*, vol. 25 (1), pp. 26-32, 2018.
- [25]. G. Çam, "Friction stir welded structural materials: Beyond Al-alloys", *Int. Mater. Rev.*, vol. 56 (1), pp. 1-48, 2011.
- [26]. G. Çam, G. İpekoğlu, T. Küçükömeroğlu, and S.M. Aktarer, "Applicability of friction stir welding to steels", *JAMME*, vol. 80(2), pp. 65-85, 2017.
- [27]. S. Selvi, A. Vishvaksenan, and E. Rajasekar, "Cold metal transfer (CMT) technology An overview", Cold metal transfer (CMT) technology An overview, *Defence Technology*, vol. 14, pp. 28-44, 2018.

[28]. G. Çam, Ç. Yeni, S. Erim, V. Ventzke, and M. Koçak, "Investigation into properties of laser welded similar and dissimilar steel joints", *Sci. Technol. Weld. Join.*, vol. 3 (4), pp. 177-189, 1998.

- [29]. J. dos Santos, G. Çam, F. Torster, A. Insfran, S. Riekehr, V. Ventzke, and M. Koçak, "Properties of power beam welded steels, Al- and Ti-alloys: Significance of strength mismatch", *Welding in the World*, vol. 44 (6), pp. 42-64, 2000.
- [30]. G. Çam, M. Koçak, and J.F. dos Santos, "Developments in laser welding of metallic materials and characterization of the joints", *Welding in the World*, vol. 43 (2), pp. 13-26, 1999.
- [31]. G. Çam, et al., "Characterization of laser and electron beam welded Al-alloys", *Prakt. Metallogr.*, vol. 36 (2), pp. 59-89, 1999.
- [32]. G. Çam and M. Koçak, "Microstructural and mechanical characterization of electron beam welded Al-alloy 7020", *J. Mater. Sci.*, vol. 42 (17), pp. 7154-7161, 2007.
- [33]. G. Çam, V. Ventzke, J.F. dos Santos, M. Koçak, G. Jennequin, and P. Gonthier-Maurin, "Characterisation of electron beam welded aluminium alloys", *Sci. Technol. Weld. Join.*, vol. 4 (5), pp. 317-323, 1999.
- [34]. T. Küçükömeroğlu, et al., "Investigation of mechanical and microstructural properties of friction stir welded dual phase (DP) steel", *IOP Conf. Series: Mater. Sci. Eng.*, vol. 629, Paper No. 012010, 2019.
- [35]. G. İpekoğlu, T. Küçükömeroğlu, S.M. Aktarer, D.M. Sekban, and G. Çam, "Investigation of microstructure and mechanical properties of friction stir welded dissimilar St37/St52 joints", *Materials Research Express*, vol. 6 (4), Article Number: 046537, 2019.
- [36]. T. Küçükömeroğlu, S.M. Aktarer, G. İpekoğlu, and G. Çam, "Mechanical properties of friction stir welded St 37 and St 44 steel joints", *Materials Testing*, vol. 60 (12), pp. 1163-1170, 2018.
- [37]. T. Küçükömeroğlu, S.M. Aktarer, G. İpekoğlu, and G. Çam, "Microstructure and mechanical properties of friction stir welded St52 steel joints", *International Journal of Minerals, Metallurgy and Materials*, vol. 25 (12), pp. 1457-1464, 2018.
- [38]. L. Cui, H. Fujii, N. Tsuji, and K. Nogi, "Friction stir welding of a high carbon steel", *Scripta Mater.*, vol. 56, pp. 637-40, 2007.
- [39]. Y. Azuma, Y. Kameno, and T. Takasugi, "Friction stir welding in stainless steel sheet of type 430 using Ni-based dual two-phase intermetallic alloy tool", *Welding International*, vol. 27 (12), pp. 929-935, 2013.
- [40]. B.W. Ahn, D.H. Choi, D.J. Kim, and S.B. Jung, "Microstructures and properties of friction stir welded 409 L stainless steel using a Si3N4 tool", *Mater. Sci. Eng. A*, vol. 532, pp. 476-479, 2012.
- [41]. A.K. Lakshminarayanan, V. Balasubramanian, "An assessment of microstructure, hardness, tensile and impact strength of friction stir welded ferritic stainless steel joints", Mater. Des., vol. 31, pp. 4592-4600, 2010.
- [42]. M.S. Khorrami, et al., "Study on microstructure and mechanical characteristics of low-carbon steel and ferritic stainless steel joints", *Materials Science & Engineering A*, vol. 608, pp. 35-45, 2014.
- [43]. M. van Warmelo, D. Nolan, and J. Norrish, "Mitigation of sensitisation effects in unstabilised 12%Cr ferritic stainless steel welds", *Materials Science & Engineering A*, vol. 464, pp. 157-169, 2007.
- [44]. G. İpekoğlu and G. Çam, "Formation of weld defects in cold metal transfer arc welded 7075-T6 plates and its effect on joint performance", *IOP Conf. Series: Materials Science and Engineering*, vol. 629, Paper No: 012007, 2019.
- [45]. M. Pakdil, G. Çam, M. Koçak, and S. Erim, "Microstructural and mechanical characterization of laser beam welded AA6056 Al-alloy", *Mater. Sci. Eng. A*, vol. 528 (24), pp. 7350-7356, 2011.
- [46]. Y. Bozkurt, S. Salman, and G. Çam, "Effect of welding parameters on lap-shear tensile properties of dissimilar friction stir spot welded AA5754-H22/2024-T3 joints", *Sci. Technol. Weld. Join.*, vol. 18 (4), pp. 337-345, 2013.
- [47]. G. İpekoğlu and G. Çam, "Effects of initial temper condition and postweld heat treatment on the properties of dissimilar friction-stir-welded joints between AA7075 and AA6061 aluminum alloys", *Metall. Mater. Trans. A*, 2014, Vol. 45A (7), pp. 3074-3087
- [48]. G. İpekoğlu, S. Erim, and G. Çam, "Investigation into the influence of post-weld heat treatment on the friction stir welded AA6061 Al-alloy plates with different temper conditions", *Metall. Mater. Trans. A*, vol. 45A (2), pp. 864-877, 2014.
- [49]. G. İpekoğlu, S. Erim, and G. Çam: "Effects of temper condition and post weld heat treatment on the microstructure and mechanical properties of friction stir butt welded AA7075 Al-alloy plates", *Int. J. Adv. Manuf. Technol.*, vol. 70 (1), pp. 201-213, 2014.
- [50]. M. Koçak, M. Pakdil, and G. Çam, "Fracture behaviour of diffusion bonded Ti-alloys with strength mismatch", *Sci. Technol. Weld. Join.*, vol. 7 (4), pp. 187-196, 2002.
- [51]. G. Çam, M. Koçak, D. Dobi, L. Heikinheimo, and M. Siren, "Fracture behaviour of diffusion bonded bimaterial Ti-Al joints", *Sci. Technol. Weld. Join.*, vol. 2 (3), pp. 95-101, 1997.